Effects of pressure on the non-linear viscoelastic behaviour of polymers: 1. Polypropylene

S. H. Joseph* and R. A. Duckett
Department of Physics, University of Leeds, Leeds LS2 9JT, UK
(Received 27 October 1977; revised 21 February 1978)

A comprehensive study of the pressure and strain rate dependence of the room temperature shear stress strain behaviour of isotropic polypropylene is described. The maximum (yield) stress is observed to increase smoothly with increasing pressure and strain rate in the pressure regime where the 1% shear modulus is passing through the main β relaxation. This indicates the differing roles of the crystalline and amorphous regions of the material at large and small strains. A modified Ree–Eyring model is shown to describe well the pressure and strain rate dependence of the maximum stress data but is inadequate to describe corresponding features of the small strain results. A semiquantitative viscoelastic analysis is used to delineate several types of non-linear behaviour at different strain and pressure levels indicating the complexity of the mechanical response of a semicrystalline polymer.

INTRODUCTION

Previous work on the effects of pressure on the mechanical properties of polymers has usually been concerned with either changes in the linear viscoelastic behaviour due to shifts of relaxation transitions with temperature and pressure, or with phenomenological measurements of increases in yield stress under high pressures. It must in principle be possible to draw together these separate approaches in a study of the effects of pressure on the non-linear viscoelastic response of the material. Our study attempts to do so in two parts: in this first part we deal with polypropylene (PP), a widely used semicrystalline engineering thermoplastic. In the second part[1] we will examine poly(vinyl acetate) (PVAC), favoured in the more fundamental investigations into the effects of temperature[2,3] and pressure[3,4] on the glass transition process.

The effects of applied hydrostatic pressure on polymers are often viewed as similar to a drop in temperature. Thus, for example, the application of hydrostatic pressure would result in a reduction of the free volume; this, together with the consequent change in material properties, could be reproduced by lowering the temperature. The equivalence of the two effects is undoubtedly not exact, but many studies have shown its usefulness and have resulted in the evaluation of pressure–temperature coefficients for shifts in the dilatometric glass transition[6], dynamic–mechanical loss maxima[7], dielectric loss maxima[4], etc. These in turn have been discussed in terms of the thermodynamics of the glass transition, and of the WLF equation[4,5]. A full list of references is to be found in the review on the subject by Jones-Parry and Tabor[8].

In the field of larger deformations the effects of pressure on polymers have been viewed as entering into a three-dimensional Green–Rivlin expansion of the non-linear viscoelastic response[9,10], as introducing a pressure term in the Eyring flow equation for the yield stress[11,12] or as a modification of the conventional formalism of pressure-independent plasticity[13,14].

In this work we have performed torsion tests on isotropic polypropylene under superimposed hydrostatic pressure at different strain rates. This has enabled the location of the mechanical loss maximum corresponding to the β transition for small deformations (modulus measurements) and the evaluation of the changes with pressure in the rate dependence of maximum stress. These are then compared and discussed in terms of the whole stress–strain–time response.

EXPERIMENTAL

Apparatus

The apparatus used is based on the torsion testing machine employed by Rabinowitz, Ward and Parry[13], modified in order to make measurements at different strain rates and temperatures, and is shown in *Figure 1*. Twist is applied to the specimen D via a shaft C which enters the balanced pressure vessels through the Morrison seals A. The shaft is

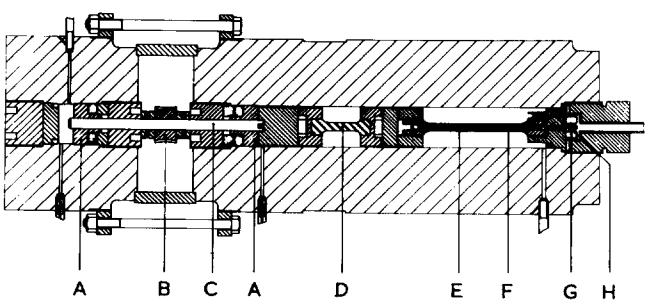

Figure 1 General view of high pressure torsion machine, see text for details

* Present address: Department of Mechanical Engineering, Imperial College, London SW7, UK.

0032–3861/78/1907–0837$02.00

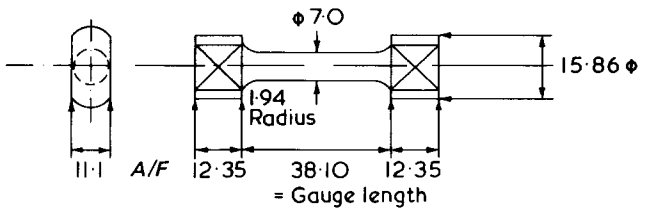

Figure 2 Specimen geometry, dimensions in mm

driven by a servo-controlled motor through a worm gear B and interchangeable gearboxes with an electromagnetic clutch-coupling, giving twist rates of between 6×10^{-1} sec^{-1} and 6×10^{-6} sec^{-1} stable to within ±5% under full load. Twist is measured by a 10 turn potentiometer coupled to the drive shaft, taking into account the machine deflection as measured with a steel bar in place of the test specimen. Torque in the specimen is measured from the deflection of a torque bar E using an angular transducer. This consists of a stator G mounted at the fixed end of the torque tube and a rotor H coupled to the specimen end of the torque bar via a steel stalk F and enables continuous monitoring of torque to an accuracy of ±2%. Specimen design (*Figure 2*) is such as to optimize the accuracy of strain measurement. The flared end sections are made as short as possible whilst remaining compatible with a low stress concentration factor in those sections (estimated to be about 1.2 for this design), and the dimensions calculated so that the effective gauge length of the specimen in the linear regime is equal to the length between the shoulders. This calculation was checked by direct measurement of twist in the central section of the specimen under pressure using a specially constructed capacitative rotometer[15]. The maximum error in strain measurement was found to be −5%, due to non-linearity of material behaviour for the effective gauge length calculation. Electrical signals corresponding to the torque and twist levels are fed into an $X-Y$ recorder and also in digital form to a paper tape punch in order to facilitate the computation of stress–strain data as described below.

Hydrostatic pressure is maintained constant to within 6 MN/m^2 peak to peak, using a hydraulic pump, 20:1 intensifier and 4-way solenoid valve, servo-controlled from a manganin cell pressure sensor. The pressure medium is Plexol 201 (diethyl dihexyl sebacate), a low temperature lubricant. Temperature is controlled by a water bath surrounding the central portion of the vessel; temperature can be varied between 10° and 90°C and controlled to ±0.3°C. Temperature is measured inside the vessel from the change in resistance in a coil of copper wire mounted in the specimen grips.

Analysis of results

In a state of pure torsion the principal strain invariants are identical to those of simple shear if we put:

$$\gamma = r\phi$$

where γ is the engineering shear strain, r is the radial distance from the cylinder axis and ϕ is the angle of twist per unit length along the axis.

Under the experimental conditions of zero axial load the deformation at non-vanishing strains will not be that of pure torsion. An estimate of the error due to this second order effect indicates that it is negligible at the shear strains (below 30%) used here. We proceed to derive stress–strain curves in simple shear on this basis. The result derived by Nadai[15] for the torsion of non-linear elastic–plastic materials may be rigorously extended to viscoelastic materials[14]. The result, assuming an homogeneous deformation is:

$$\tau(\gamma_b) = \frac{1}{2\pi}\left[\frac{3M}{b^3} + \gamma_b \frac{\partial}{\partial \gamma_b}\left(\frac{M}{b^3}\right)_{\dot{\gamma}_b} + \frac{\partial}{\partial(\ln \dot{\gamma}_b)}\left(\frac{M}{b^3}\right)_{\gamma_b}\right] \quad (1)$$

where $\tau(\gamma_b)$ is the shear stress at strain = γ_b; b is the radius of cylindrical specimen, M is the torque applied to the specimen; γ_b is the shear strain at surface of cylinder, where $r = b$; $\dot{\gamma}_b$ is the shear strain rate at $r = b$.

This expression is applied to the torque–twist data output from the apparatus to give stress–strain curves at constant strain rate. 'Isochronal' curves (stress vs. strain at constant time) are constructed from the stress–strain curves by interpolation between constant strain rate curves.

Material and tests run

The polypropylene was a commercial isotactic homopolymer, melt extruded into rods 40 mm in diameter. It was annealed at 120°C for 20 min after extrusion, and proved to be in an 'early wheatsheaf' stage of spherulite growth upon examination under the optical microscope. The density was 909.5 kg/m^3. The specimen design of *Figure 2* was machined at high cutting speed using plenty of coolant. Specimens were stored at room temperature (22°C) and humidity (60% r.h.) until testing.

Constant twist rate tests at 21°C at strain rates equivalent to between 5×10^{-5} and 5×10^{-2} sec^{-1} were performed at five pressures from 1 atm to 450 MN/m^2 at strains of up to 20%. The results are shown in *Figures 3–9*.

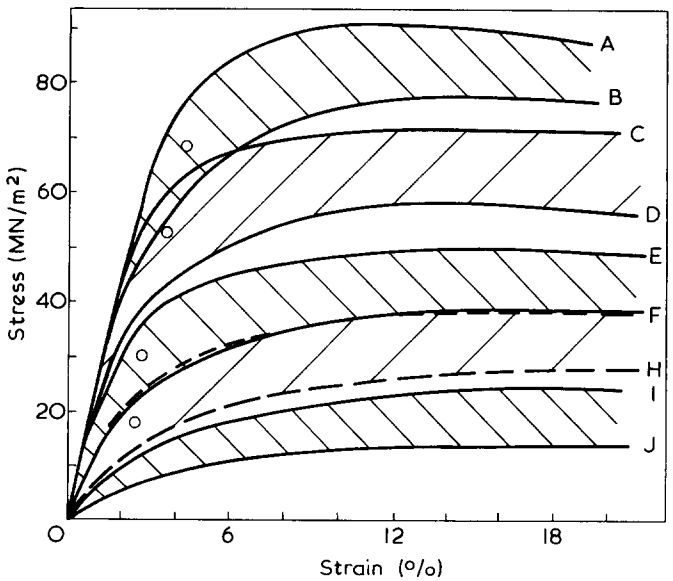

Figure 3 Constant strain rate stress–strain curves for polypropylene at 21°C. Two curves are shown corresponding to the maximum and minimum strain rates at each pressure used. ⊙ peaks in $y = d\ln\tau/d\ln t|_\gamma$ from *Figure 14*. A, pressure 450 MN/m^2, ln (strain rate) −3.0; B, pressure 450 MN/m^2, ln (strain rate) −10.3; C, pressure 300 MN/m^2, ln (strain rate) −3.0; D, pressure 300 MN/m^2, ln (strain rate) −10.3; E, pressure 150 MN/m^2, ln (strain rate) −2.9; F, pressure 150 MN/m^2, ln (strain rate) −10.3; G, pressure 75 MN/m^2, ln (strain rate) −2.9; H, pressure 75 MN/m^2 ln (strain rate) −10.3; I, pressure 0.1 MN/m^2, ln (strain rate) −2.9; J, pressure 0.1 MN/m^2, ln (strain rate) −10.5

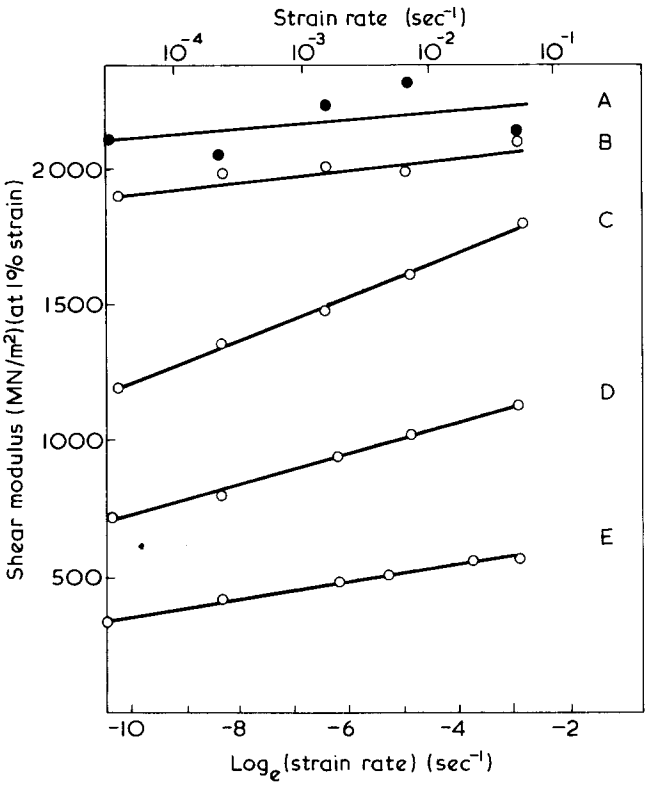

Figure 4 Shear modulus (1% strain) of polypropylene at 21°C, showing dependence on strain rate at each pressure. Pressure (MN/m^2): A, 450; B, 300; C, 150; D, 75; E, 0.1

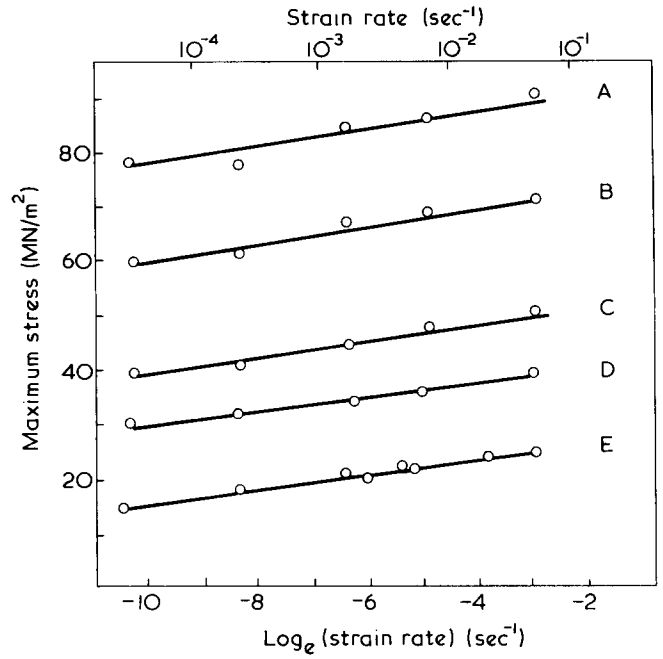

Figure 5 Maximum stress for polypropylene at 21°C, showing the strain rate dependence at each pressure. Pressure (MN/m^2): A, 450; B, 300; C, 150; D, 75; E, 0.1

RESULTS AND DISCUSSIONS

Preliminary observations

Much basic information can be deduced from an examination of the general form of these results shown in *Figure 3*. *Figures 4* and *5* show the strain rate dependence of both modulus and maximum stress, respectively, and the large changes in both brought about by the application of 450 MN/m^2 pressure. The maximum stress rises from about 20 to 85 MN/m^2, and the modulus increases from 450 to 2150 MN/m^2 in this pressure range. Looking at the effects of pressure on the modulus we see that the variation with pressure is sigmoidal (see *Figure 6*) and that in the region of most rapid variation of modulus with pressure (at about

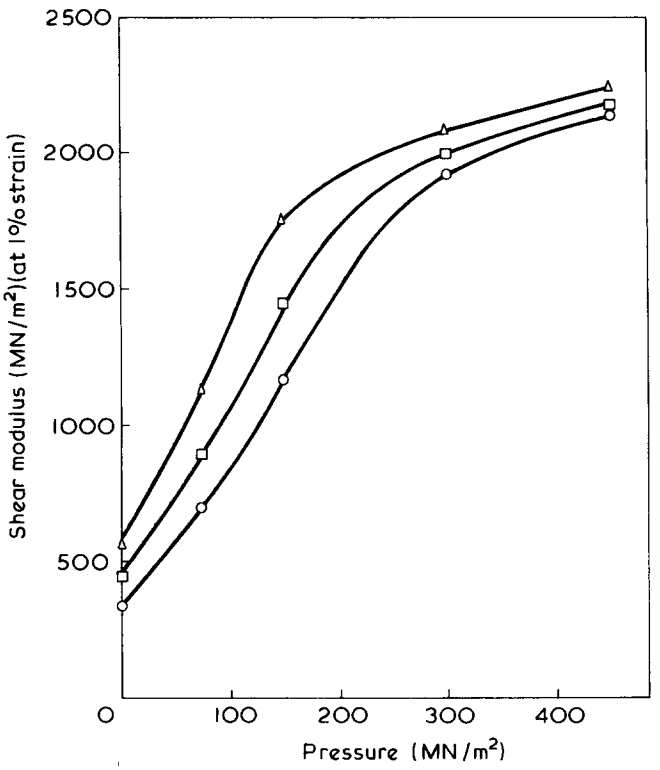

Figure 6 Shear modulus (1% strain) showing pressure dependence at the strain rates: △, 5 x 10^{-2} sec^{-1}; □, 9.1 x 10^{-4} sec^{-1}; ○, 2.75 x 10^{-5} sec^{-1}

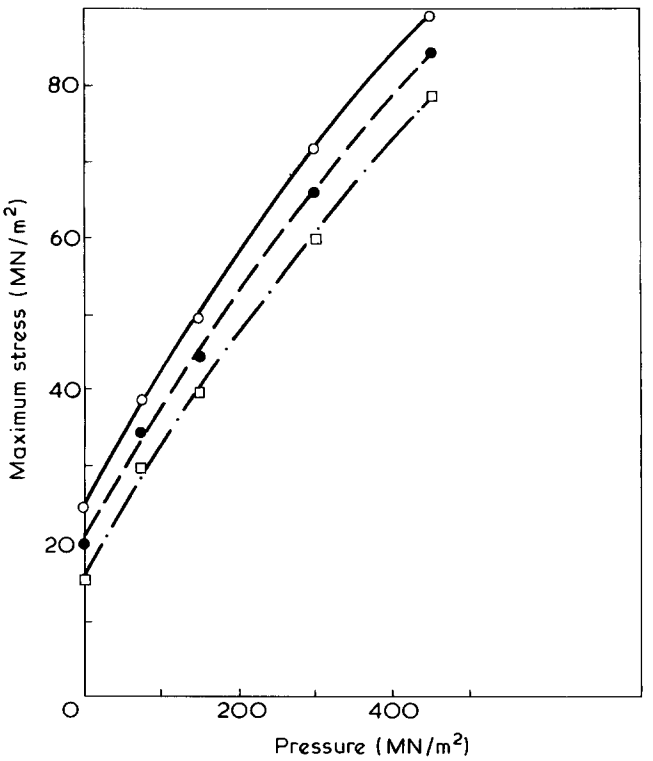

Figure 7 Maximum stress *versus* pressure. Strain rates: ○, 5 x 10^{-2} sec^{-1}; ●, 1.66 x 10^{-3} sec^{-1}; □, 4.5 x 10^{-5} sec^{-1}

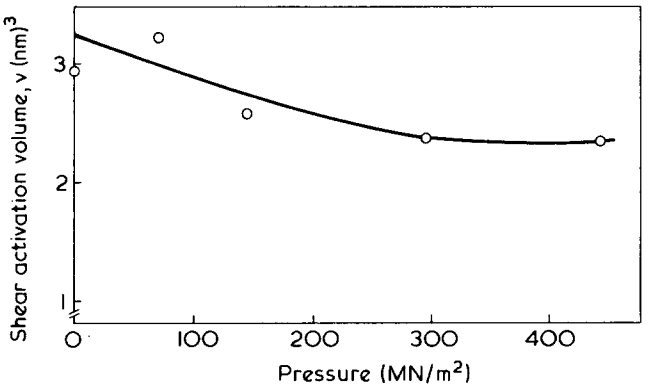

Figure 8 Pressure dependence of the shear activation volume, v (calculated from *Figure 5*, see text)

150 MN/m^2) the modulus is also most rate dependent (see *Figure 4*). This is consistent with the interpretation that the application of pressure brings about the β transition in the material. It is generally agreed[16] that this β transition is the glass–rubber transition in the amorphous regions. The β transition for PP has been found to produce a peak in the loss tangent in torsion pendulum measurements at about 1 Hz at temperatures between 2° and 7°C at atmospheric pressure for specimens of similar crystallinity to those used here[6,7]. The position of this loss peak on the temperature scale has been found to shift with applied pressure by about 0.09°C (MN/m^2)$^{-1}$ [7], so we would expect that the sigmoidal variation of shear modulus observed as temperature is reduced will be reproduced under the application of pressure, and also that the rate dependence of modulus should show a maximum as pressure increases, corresponding to the damping maximum in the torsion pendulum data.

Figure 7 shows that the maximum stress, τ_m, increases non-linearly with pressure, P, i.e. $d\tau_m/dP$ decreases as P increases. *Figure 5* shows that the strain rate dependence of τ_m increases slightly as pressure increases: if $\dot{\gamma}$ = strain rate, then $d\tau_m/d(\ln\dot{\gamma})$ changes from 1.38 to 1.75 MN/m^2 as P increases from 1 atm to 450 MN/m^2. *Figure 3* indicates that at atmospheric pressure the stress is still rising slowly at the highest strain level reached in the test. Thus values of τ_m estimated from these results will not be those of true maximum stress. We shall however continue to use these values to approximate to the yield stress.)

β transition

As stated above, the variations of modulus with pressure and with strain rate indicate the presence of a relaxation transition at 21°C in the region of 150 MN/m^2 pressure and at a strain rate of 10^{-3} sec^{-1}. To compare this with the torsion pendulum data of ref 7 we represent the material by a linear viscoelastic system with a spectrum of relaxation times, θ, with a peak in the spectrum at $\theta = \theta_m$. In the Alfrey approximation it is readily shown that if:

$$S = \left.\frac{\partial G}{\partial(\ln\dot{\gamma})}\right|_{\gamma}$$

where $G = G(\gamma,\dot{\gamma})$ = shear modulus, then S is maximal, i.e. $S = S_{max}$ at $\gamma/\dot{\gamma} = 1.8\theta_m$. The data of *Figure 5* thus show that $\theta_m \approx 5$ sec at 21°C and 150 MN/m^2 pressure. Exact comparison with other data is rendered difficult by the dependence of the temperature of the β damping peak on crystallinity as shown by Passaglia *et al.*[6] and Flocke[17] but comparison of their torsion pendulum data with the data in ref 7 would however suggest that $\theta_m = 0.1$ sec at 12°C and 130 MN/m^2 pressure, which is reasonably consistent with our results. The quantity S_{max} is also a measure of the sharpness of the transition: we find here that S_{max} for polypropylene (S^{PP}_{max}) is much smaller than S_{max} for a single relaxation time (S^{sr}_{max}):

$$S^{PP}_{max} = 0.145\, S^{sr}_{max}$$

indicating a broad spread of relaxation times, and justifying the use of the Alfrey approximation above. We may also use the S_{max} value to predict the peak value of the imaginary part of the complex modulus at the β transition, G''_{max}, thence to compare with the torsion pendulum loss peak using a method due to Tuijmann[19].

This gives $G''_{max} = 200$ MN/m^2 at 21°C, 150 MN/m^2 pressure and 0.03 Hz compared with $G''_{max} = 70$ MN/m^2 at 2°C, atmospheric pressure and 1 Hz as found by Passaglia and Martin[6]. Thus the transition induced by pressure at 21°C is sharper than that induced by lowering the temperature to 2°C. This may correspond to the broadening of transitions observed in dielectric studies as temperature is lowered[16], and would indicate that this braodening is a result of lowering temperature that cannot be reproduced by applied pressure.

Yield behaviour

The graphs of yield or maximum stress τ_m (*Figure 5*) are linear with $\ln\dot{\gamma}$ and are therefore consistent with the assumption that the Eyring flow equation holds when $\tau = \tau_m$. This equation in the modified form due to Ward[11], reads:

$$\dot{\gamma} = A\exp\frac{-(\Delta U - \tau_m v + P\Omega)}{k_B T} \qquad (2)$$

where A is a constant; v is the shear activation volume; ΔU is the activation energy; Ω is the pressure activation volume; k_B is the Boltzmann constant and T the temperature.

Graphs of v and Ω against pressure derived on the basis of equation (2) are shown in *Figures 8* and *9*. Evidently, both shear and pressure activation volumes decrease slightly with pressure as would be expected if these parameters represent a physical volume in the material. A 'bulk compliance' from the pressure dependence of both v and Ω can be estimated and is found to be approximately 1.0 (GN/m^2)$^{-1}$ in both

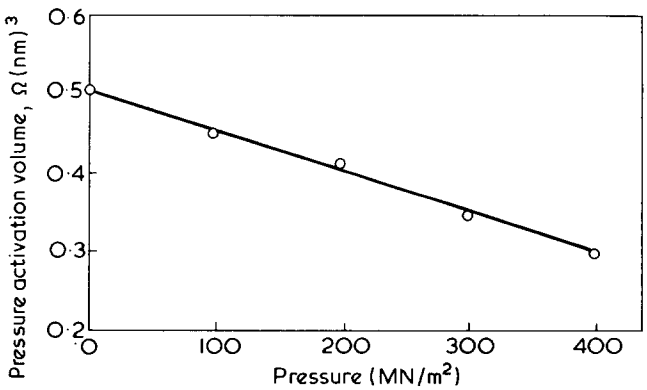

Figure 9 Pressure dependence of the pressure activation volume, Ω (calculated from *Figure 5*, see text)

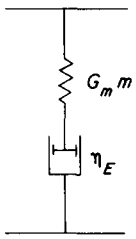

Figure 10 Non-linear Maxwell element with spring stiffness G_m, Eyring dashpot viscosity η_E

cases. This is about three times the value of the macroscopic bulk compliance of PP at low pressures[19]. If we treat the material as a simple composite material, then the macroscopic bulk compliance can be written approximately as:

$$\beta = (1 - f_c)\beta_a + v_c\beta_c$$

where f_c is the volume fraction of crystals which are assumed to have a compressibility β_c, and β_a is the compressibility of the amorphous phase. In our case, the crystallinity f_c is approximately 67%. If we assume that this is also true for the samples in ref 19 and that β_c is effectively zero, then these data imply a compressibility of the amorphous phase $\beta_a \sim 1(\mathrm{GN/m^2})^{-1}$, compatible with the variation of activation volumes with pressure measured here. This is consistent with the view[20] that the regions of the material undergoing yield are in a state of disorder similar to that of an amorphous rubbery polymer.

Comparison of yield and modulus results

In view of the success obtained by Bauwens *et al.*[20,21] relating, by means of the Ree–Eyring equation, the relaxation transitions observed in small strain experiments on polycarbonate and poly(methyl methacrylate) to aspects of the rate dependence of the yield stress, and of the use of this equation for the interpretation of the effects of pressure on the yield stress of polypropylene[11], we have tested its applicability to our results. The method uses one or more viscous elements obeying the following equations:

$$\dot{\gamma} = 2A\exp\frac{-(\Delta U + P\Omega)}{k_BT}\sinh\frac{\tau v}{k_BT} \qquad (3)$$

where the variables are as defined above.

This can be written, at constant temperature and pressure, as:

$$\dot{\gamma} = \dot{\gamma}_0\sinh(\tau/\tau_0) \qquad (4)$$

where $\dot{\gamma}_0$ and τ_0 are the new constants. Comparison of equations (2) and (3) in the limit of high stresses, $\tau/\tau_0 \gg 1$, reveals that $\tau_0 = k_BT/v$ and is therefore determined by the strain rate dependence of the yield stress. If $\tau \ll \tau_0$, then:

$$\dot{\gamma} = (\tau/\tau_0)\dot{\gamma}(P) \qquad (5)$$

which is a linear viscous response.

For $\tau \gg \tau_0$:

$$\dot{\gamma} = \tfrac{1}{2}\dot{\gamma}_0(P)\exp(\tau/\tau_0) \qquad (6)$$

as in equation (2). If we incorporate this viscous unit with a spring of stiffness G_m into a Maxwell type element as in *Figure 10* where:

$$\eta_e(\tau) = \tau/\dot{\gamma} \qquad (7)$$

then we have a non-linear element with a relaxation time at small stresses given by:

$$\theta_m = \eta_e(0)/G_m = \tau_0/[\dot{\gamma}_0(P)G_m] \qquad (8)$$

Thus, for this system the linear viscoelastic relaxation time may be calculated from the parameters τ_0 and $\dot{\gamma}_0(P)$, which are in turn determined by the maximum stress data. Firstly we use the maximum stress data of *Figure 5* to evaluate the shifts in τ_0 and $\dot{\gamma}_0$ with pressure, and so, using equation (8), we can calculate the expected changes in the *linear* relaxation time with pressure. These calculated values are compared in *Figure 11* with values deduced from the shear modulus data of *Figure 4*, assuming that the shifts are due entirely to changes in θ_m with pressure. Agreement appears poor, but is acceptable if we consider: (1) that the quantities involved are all derivatives of experimental values and are thus particularly subject to error; (2) that the two plots are derived from quite different parts of the stress–strain curve; and (3) that only simple horizontal shifts of the modulus data have been used.

We conclude that the changes in the rate dependence of both yield stress and modulus can be described by the Ree–Eyring equation incorporating a single function of pressure.

So far only the shifts of relaxation time with pressure have been compared at high and low strains; the absolute values of relaxation time remain to be examined. In this latter case the Ree–Eyring equation is not so successful, as is seen most clearly by the examination of the dependence of yield stress on strain rate, given by this equation as shown in *Figure 12*. For simplicity the response of only one element is shown, this then represents the addition to the yield stress due to the onset of the β transition. The regions of the response described by equations (5) and (6) are indicated. The x-axis is, in practice, that of extended strain rate derived, for instance, from the results of tests at different values of P

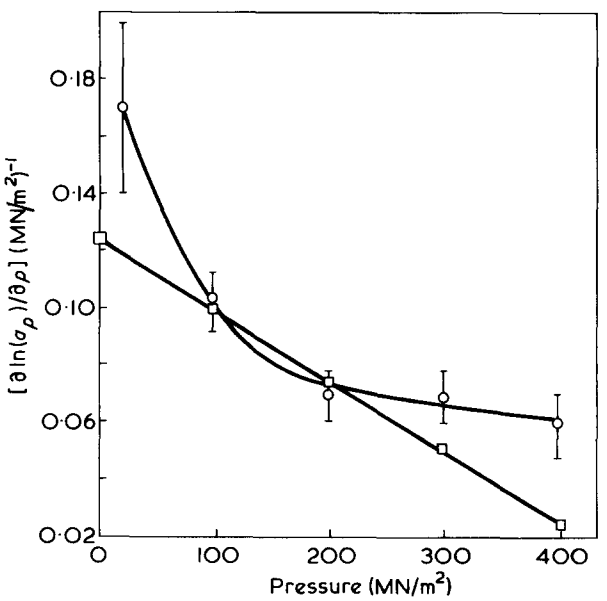

Figure 11 The pressure dependence of the shift factor $\ln(a_p)$ from maximum stress data, from small strain data

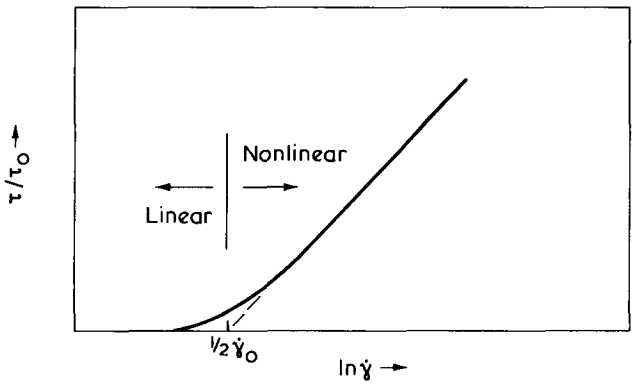

Figure 12 Maximum stress behaviour expected from the Ree–Eyring model

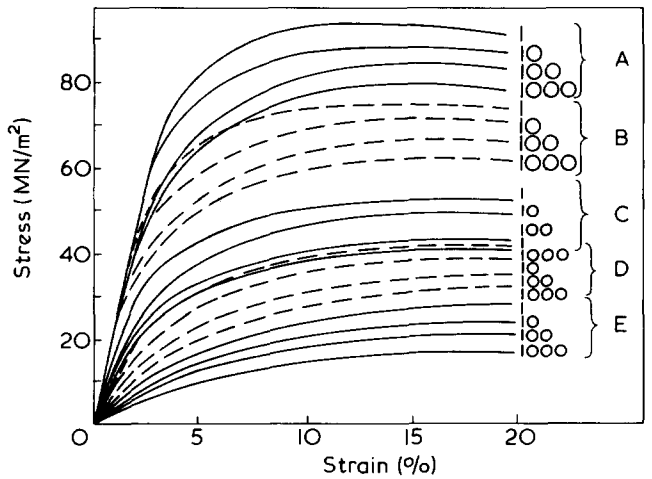

Figure 13 Isochronal stress–strain curves, numerically interpolated from the data in *Figure 3*. Four curves at each pressure corresponding to t = 1, 10, 100 and 1000 sec. Pressure (MN/m^2): A, 450; B, 300; C, 150; D, 75; E, 0.1

that have been shifted to form a composite curve. *Figure 12* shows that the existence of a relaxation transition in the linear response should be accompanied by a change in the gradient of this composite yield stress curve at the appropriate strain rate and pressure. One equally expects an increase in gradient in the graphs of maximum stress vs. pressure as the transition pressure is traversed.

Neither of these expectations is fulfilled; the slight change in rate dependence of yield stress from atmospheric pressure to 450 MN/m^2 shown in *Figures 5* and *8* is quite inadequate to explain these data on the basis of the Ree–Eyring equation, and the maximum stress curves in *Figure 7* even show a continuous decrease in slope through the transition. This discrepancy also appears in the data of ref 12 on polypropylene. Furthermore, values of relaxation time calculated from equation (8) disagree with those found from the modulus results by several orders of magnitude. We thus conclude that the deformation of polypropylene under pressure is not well described by the Ree–Eyring equation using the same set of parameters for both low and high strain measurements.

Variation of the time-dependent response with strain

A more formal study of the mechanical behaviour takes as its starting point the basic stress–strain data presented in *Figure 3*. These data are replotted in *Figure 13* as a set of isochronal stress–strain curves at each pressure. It is apparent that the time dependence of the stress varies with strain and that this variation has different characteristics at the different pressures. This may be examined by analysis of the expression:

$$y = -\frac{\mathrm{d}(\ln\tau)}{\mathrm{d}(\ln t)} \qquad \gamma = \text{constant}$$

as a function of strain. For a *linear* system y would be independent of strain, and would be a maximum when $t \sim \theta_m$ i.e. in the region of a relaxation transition. In *Figure 14*, values of y derived from the isochronal data of *Figure 13* are plotted *versus* strain at each of the pressures investigated. Throughout the range of the present data, y is found to be independent of time, t, an observation consistent with the breadth of relaxation times deduced from the low strain data. It is seen that y is small at high pressures and small strains, corresponding to the rate independence of the small strain modulus at those pressures. At intermediate pressures a peak in y develops which becomes sharper and higher as the pressure is lowered. The strain γ_m at which y is a maximum is marked in *Figure 3*. It appears that γ_m is located near a region of high curvature on the stress–strain curve, but it is not possible to locate this region of high curvature more precisely by differentiation of the stress–strain data because of experimental scatter.

We might liken the peak in y to the peak in the loss modulus observed near a relaxation transition. The peak may locate the levels of stress and strain at which the activated processes in the material have a rate approximately equal to the experimental rate. The levels of both strain and stress at which y is a peak rise as the pressure rises: this is consistent with the view that as the small strain relaxation

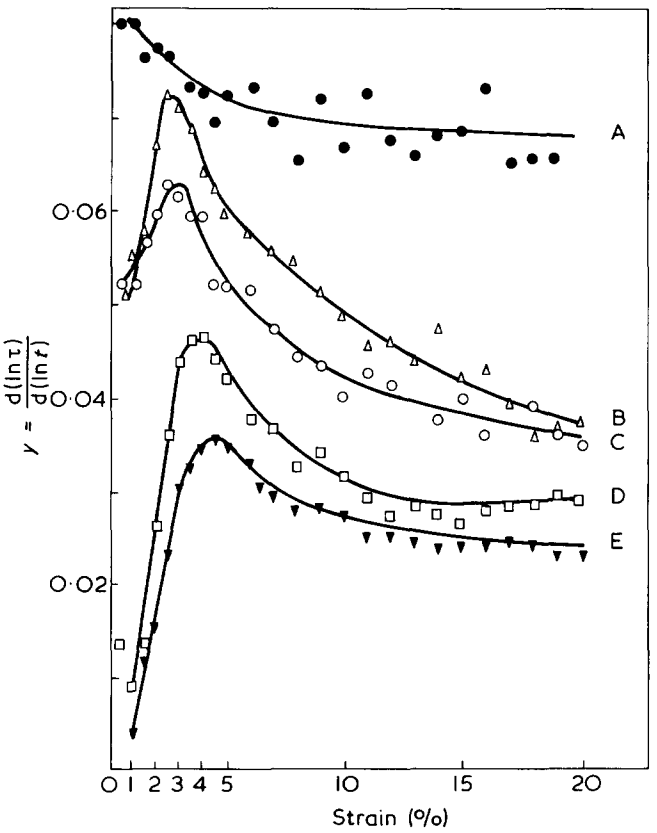

Figure 14 Relative time dependence of the shear stress d(lnτ)/(dln$t$) *versus* strain at each pressure level. Pressure (MN/m^2): A, 0.1; B, 75; C, 150; D, 300; E, 450

time becomes longer, so the stress required to activate the process to the experimental rate becomes higher. The stress–strain curves indicate also, unlike the case of glassy polymers, that subsequent to the maximum in y the stress continues to rise before levelling off. It may thus be possible to break up the curve into regions where different processes dominate as follows. Consider the curves for $P = 300$ MN/m^2 in *Figure 3:*

Let the range $0 < \gamma < 0.038$ be region X;
Let the range $0.038 < \gamma > 0.090$ be region Y;
Let the range $0.090 < \gamma$ be region Z.

In region X the stress is mainly controlled by the β process in the amorphous areas. At the border between X and Y the yield process of the amorphous regions is setting in, as marked by the peak in rate dependence shown in *Figure 14*. The increase of stress in region Y is due mainly to the resistance of the crystalline areas of the polymer. In region Z the material flows at constant stress. If the curves of *Figure 3* are now examined at the different pressures, it is seen that as the pressure is lowered, region X disappears completely, and region Y spreads out to embrace the entire curve. This is consistent with the fact that as the pressure drops so the amorphous areas become mobile, and that the stiffness and strength at atmospheric pressure are mainly controlled by the crystallinity.

CONCLUSIONS

These torsion tests on polypropylene show the need to take into account relaxation transitions and morphology when attempting any description of the non-linear viscoelastic behaviour of polymers. The changes in shear modulus can be described by shifts in relaxation time under pressure, and those in yield stress by a pressure modified Eyring flow equation. An attempt to link these two successes in a simple model failed, and a more complex scheme to explain this has been proposed: this scheme is qualitative and tentative. The characteristics of the material are determined by a complex interaction between crystalline and amorphous areas in the material, and this sort of scheme can only begin to indicate the interplay of structures and processes. In order to be able to verify properly the scheme we should need data from samples of polypropylene different both in morphology and crystallinity.

It does however show the importance of considering the multiplicity of processes present, and that the evaluation of material parameters from modulus or maximum stress results in isolation may not be confirmed by the examination of behaviour at intermediate strain levels.

In the second part of this study[1] we report work on PVAC, in which the α transition is examined; this transition dominates the behaviour of the material over a considerable range of temperature, which thus prevents a clearer picture of the effects of such a transition on its mechanical properties.

REFERENCES

1 Joseph, S. H. and Duckett, R. A. *Polymer* 1978, **19**, 844
2 Williams, M. L. and Ferry, J. D. *J. Colloid Sci.* 1954, **9**, 479
3 Williams, M. L., Landel, R. F. and Ferry, J. D. *J. Am. Chem. Soc.* 1955, **77**, 3701
4 O'Reilly, J. M. *J. Polym. Sci.* 1962, **57**, 429
5 McKinney, J. E. and Belcher, H. V. *J. Res. Nat. Bur. Stand. (A)* 1963, **67**, 43
6 Passaglia, E. and Martin, G. M. *J. Res. Nat. Bur. Stand. (A)* 1964, **68**, 519
7 Jones-Parry, E. and Tabor, D. *Polymer* 1973, **14**, 617
8 Jones-Parry, E. and Tabor, D. *J. Mater. Sci.* 1974, **8**, 1510
9 Lockett, F. J. *Int. J. Eng. Sci.* 1965, **3**, 59
10 Lockett, F. J. 'Non-linear viscoelastic solids', Academic Press, London, 1972
11 Ward, I. M. *J. Mater. Sci.* 1971, **6**, 1397
12 Yoon, H. N., Pae, K. D. and Sauer, J. A. *J. Polym. Sci.* 1976, **14**, 1611
13 Rabinowitz, S., Ward, I. M. and Parry, J. C. S. *J. Mater. Sci.* 1970, **5**, 29
14 Joseph, S. H. *PhD Thesis* University of Leeds (1976)
15 Nadai, A. 'Theory of flow and fracture of solids', 1950, **1**, 349
16 McCrum, N. G., Read, B. E. and Williams, G. 'Anelastic and dielectric effects in polymer solids', Wiley, New York, 1967
17 Flocke, W. G. *Kolloid Z.* 1962, **180**, 118
18 Tuijmann, C. A. F. *J. Polym. Sci.* 1967, **16**, 2379
19 Mallon, P. J. and Benham, P. P. *Plast. Polym.* 1972, **40**, 77
20 Robertson, R. E. *J. Chem. Phys.* 1960, **44**, 3950
21 Bauwens-Crowet, C., Bauwens, J. C. and Homes, G. *J. Polym. Sci.* 1969, **7**, 735
22 Bauwens-Crowet, C. *J. Mater. Sci.* 1973, **8**, 968